Chinese Journal of
POLYMER SCIENCE 高分子科学

Synthesis and AO Resistant Properties of Novel Polyimide Fibers Containing Phenylphosphine Oxide Groups in Main Chain

Zhao Yong, Gao Hong, Li Guo-Min, Liu Fang-Fang, Dai Xue-Min, Dong Zhi-Xin, Qiu Xue-Peng

Cite this article as:
Zhao Yong, Gao Hong, Li Guo-Min, Liu Fang-Fang, Dai Xue-Min, Dong Zhi-Xin, Qiu Xue-Peng. Synthesis and AO Resistant Properties of Novel Polyimide Fibers Containing Phenylphosphine Oxide Groups in Main Chain[J]. *Chinese J. Polym. Sci*, 2019, 37(1): 59-67. doi: 10.1007/s10118-019-2179-2

View online: https://doi.org/10.1007/s10118-019-2179-2

Articles you may be interested in

AO-resistant Properties of Polyimide Fibers Containing Phosphorous Groups in Main Chains
Chinese J. Polym. Sci. 2016, 34(12): 1469 https://doi.org/10.1007/s10118-016-1864-7

Synthesis and Properties of Novel Polyimide Fibers Containing Phosphorus Groups in the Side Chain (DATPPO)
Chinese J. Polym. Sci. 2017, 35(3): 372 https://doi.org/10.1007/s10118-017-1896-7

Mechanical Properties of Polyimide/Multi-walled Carbon Nanotube Composite Fibers
Chinese J. Polym. Sci. 2016, 34(11): 1386 https://doi.org/10.1007/s10118-016-1841-1

一种主链含光敏基团聚酰亚胺的合成与表征
SYNTHESIS AND CHARACTERIZATION OF POLYIMIDE WITH MAINCHAIN PHOTOSENSITIVE GROUPS AND HYDROXYL SIDEGROUPS
高分子学报. 2008(11): 1113 https://doi.org/10.3724/SP.J.1105.2008.01113

聚酰胺酸湿法纺丝凝固过程三元相图的初步构建
The Construction of Phase Diagrams for Coagulation Formation of the Wet Spinning of Polyimide Fibers
高分子学报. 2014(2): 286 https://doi.org/10.3724/SP.J.1105.2014.13238

一种含酚酞结构聚酰亚胺的合成及性能表征
SYNTHESIS AND CHARACTERIZATION OF A POLYIMIDE CONTAINING PHENOLPHTHALEIN GROUPS
高分子学报. 2012(3): 278 https://doi.org/10.3724/SP.J.1105.2012.11180

Chinese Journal of
POLYMER SCIENCE

ARTICLE

https://doi.org/10.1007/s10118-019-2179-2
Chinese J. Polym. Sci. **2019**, *37*, 59–67

Synthesis and AO Resistant Properties of Novel Polyimide Fibers Containing Phenylphosphine Oxide Groups in Main Chain

Yong Zhao[a,b], Hong Gao[c], Guo-Min Li[a], Fang-Fang Liu[a], Xue-Min Dai[a], Zhi-Xin Dong[a*], and Xue-Peng Qiu[a*]

[a] *Polymer Composites Engineering Laboratory, Changchun Institute of Applied Chemistry, Chinese Academy of Sciences, Changchun 130022, China*
[b] *University of Chinese Academy of Sciences, Beijing 100049, China*
[c] *China Academy of Space Technology, Beijing 100094, China*

Electronic Supplementary Information

Abstract A series of co-polyimide (PI) fibers containing phenylphosphine oxide (PPO) group were synthesized by incorporating the bis(4-aminophenoxy) phenyl phosphine oxide (DAPOPPO) monomer into the PI molecular chain followed by dry-jet wet spinning. The effects of DAPOPPO molar content on the atomic oxygen (AO) resistance of the fibers were investigated systematically. When the AO fluence increased from 0 atoms·cm^{-2} to 3.2 × 10^{20} atoms·cm^{-2}, the mass loss of the fibers showed the dependence on DAPOPPO molar content in co-PI fibers. The PI fiber containing 40% DAPOPPO showed lower mass loss compared to those containing 0% and 20% DAPOPPO. At higher AO fluence, the higher DAPOPPO content gave rise to dense carpet-like surface of fibers. XPS results indicated that the passivated phosphate layer was deposited on the fiber surface when exposed to AO, which effectively prevented fiber from AO erosion. With the DAPOPPO content increasing from 0% to 40%, the retentions of tensile strength and initial modulus for the fibers exhibited obvious growth from 44% to 68%, and 59% to 70%, after AO exposure with the fluence of 3.2 × 10^{20} atoms·cm^{-2}. The excellent AO resistance benefits the fibers for application in low Earth orbit as flexible construction components.

Keywords Polyimide fibers; Bis(4-aminophenoxy) phenyl phosphine oxide (DAPOPPO); Dry-jet wet spinning; AO resistance

Citation: Zhao, Y.; Gao, H.; Li, G. M.; Liu, F. F.; Dai, X. M.; Dong, Z. X.; Qiu, X. P. Synthesis and AO resistant properties of novel polyimide fibers containing phenylphosphine oxide groups in main chain. *Chinese J. Polym. Sci.* **2019**, *37*, 59–67.

INTRODUCTION

Atomic oxygen (AO) attack to polymer materials on the surface of spacecraft in low Earth orbit (LEO, 200–700 km) is a serious problem that threatens spacecraft in-orbit safe operation and service life.[1–3] As one of critical materials, polyimide (PI) fibers and their fabrics are generally used to be flexible construction components of spacecraft installed on the external surfaces, including different fastener assemblies, tensional cables, flexible sheetings and screens, railings, and safety lines.[4–8] When suffered AO attack, the surface destroy, mass loss and degradation of the mechanical properties for the fibers would happen.[9–11]

Generally, polymer materials are protected by the deposition of a coating, often aluminum oxide, silicon dioxide, tin oxide, or indium tin oxide base, which could resist to degradation of AO. However, there are restrictions on the shape and size of polymer materials that can be coating protected. Meanwhile, the thermal expansion coefficients of these inorganic coatings show significant difference from those of polymers, leading to cracks developing during thermal cycling. Moreover, folding or bending with small radii cannot be allowed.[2,12–15] Consequently, alternative and self-regenerative methods of protection are adopted. The strategy of incorporating phenylphosphine oxide (PPO) groups into polymer chain has focused on improving the AO resistance. Connell and co-workers at NASA Langley have developed a series of PPO-containing aromatic polymers, which provides AO and oxygen plasma resistance.[16–20] It had been demonstrated that the polymers typically contained 3%–7% by weight of phosphorous exhibited high glass transition temperatures and Young's moduli. Based on those, a series of PI containing PPO groups have been prepared, which exhibit excellent AO resistance, adhesion properties to metal substrates, and miscibility with many thermoplastic and thermosetting polymers.[10,14,21–27]

Therefore, aiming to fabricate PI fibers containing PPO groups to be used in space, bis(4-aminophenoxy) phenyl phosphine oxide (DAPOPPO) was designed and synthesized. Subsequently, a series of co-PI fibers were prepared by polycondensation of the above diamine monomer with commercially available aromatic dianhydride and diamine, followed by dry-jet wet spinning. The AO resistance, morphology, thermal and mechanical properties of the co-PI fibers were investigated systemically.

* Corresponding authors: E-mail zxdong@ciac.ac.cn (Z.X.D.)
E-mail xp_q@ciac.ac.cn (X.P.Q.)

Received June 6, 2018; Accepted August 6, 2018; Published online September 7, 2018

© Chinese Chemical Society
Institute of Chemistry, Chinese Academy of Sciences
Springer-Verlag GmbH Germany, part of Springer Nature 2018

EXPERIMENTAL

Chemicals and Materials

Phenyl phosphoric dichloride (PPDC) (TCI Company, China), *p*-nitrophenol (TCI Company, China), and *N*,*N*′-dicyclohexylcarbodie (TCI Company, China) were used as received. 1,8-Diazabicyclo[5.4.0]undec-7-ene (DBU), 4,4′-oxydianiline (4,4′-ODA) and pyromellitic dianhydride (PMDA) were purchased from Shanghai Research Institute of Synthetic Resins. PMDA was dried in vacuum at 260 °C overnight prior to use. Triphenylphosphine, dichloromethane (CH_2Cl_2), petroleum ether, ethyl acetate, and *N*,*N*′-dimethyacetamide (DMAc) were purchased from Shanghai Darui Fine Chemical Co., Ltd. and used without further purification.

Monomers Synthesis

The monomer, bis(4-aminophenoxy) phenyl phosphine oxide (DAPOPPO), was synthesized according to the previous reports[28,29] with some modification and the synthesis route is shown in Scheme 1. The details are as follows.

Synthesis of bis(4-nitrophenoxy) phenyl phosphine oxide (DNPOPPO)

p-Nitrophenol (389.51 g, 2.8 mol) was stirred with 8000 mL of CH_2Cl_2 in a round-bottom flask. Distilled dry DBU (425.97 g, 2.8 mol) was added into the solution and then the solution was cooled to 0 °C in an ice bath. After adding DMAc (20 g), a solution of PPDC (288.58 g, 1.48 mol) was added into the reaction solution dropwise over a period of 1 h. After maintaining at 0 °C for 3 h, the solution was kept at room temperature for another 12 h. The reaction was monitored by TLC. After the reaction finished, the solution was washed three times by water and the organic layer was separated and collected after drying over $MgSO_4$. The organic solution was concentrated and precipitated by methanol. After filtered and washed with methanol, the final product was obtained in a 75% yield. FTIR (KBr, ν, cm^{-1}): 1517 and 1348 (Ph—NO_2), 1438 (P—Ph), 1231 (—P=O), and 860 (—C—NO_2) (As seen in Fig. S1, in electronic supplementary information, ESI).

Synthesis of bis(4-aminophenoxy) phenyl phosphine oxide (DAPOPPO)

DNPOPPO was placed in a round-bottom flask with 480.30 g of powder tin(II) chloride dehydrate. Ethyl acetate (6000 mL) was introduced into the flask equipped with a condenser. The reaction mixture was stirred at room temperature for 2 h. After the solid dissolved, the solution was stirred at 60 °C for 6 h followed by cooling to the room temperature. The solution was neutralized by saturated sodium carbonate aqueous solution. The organic layer was separated and concentrated. Finally, the product was precipitated out using the petroleum ether. The obtained solid was recrystallized by CH_2Cl_2 to afford the pure product in a 90% yield. m.p. 155–156 °C. FTIR (KBr, ν, cm^{-1}): 3448 and 3345 (Ph—NH_2), 1438 (P—Ph), and 1256 (—P=O). ^{1}H-NMR (400 MHz, DMSO-d_6, δ, ppm): 7.85 (m, 2H), 7.65 (t, 1H), 7.55 (m, 2H), 6.83 (d, 4H), 6.50 (d, 4H), 5.02 (s, 4H). ^{31}P-NMR (162 MHz, DMSO-d_6, δ, ppm): 11.96. ^{13}C-NMR (101 MHz, DMSO-d_6, δ, ppm): 145.95, 133.10, 132.08, 131.97, 128.81, 128.67, 120.81 and 114.34 (As seen in Fig. S2 in ESI). Theoretical calculation for elements of $C_{18}H_{17}N_2O_3P$ was C: 63.53%, H: 5.04%, N: 8.23%, O: 14.10%, P: 9.10%. Found elemental contents were C: 56.89%, H: 4.48%, P: 7.60%.

Synthesis of Poly(amic acid) (PAA) Spinning Solutions

Using the high purity diamine monomer (DAPOPPO), we had successfully synthesized a series of phosphorous-containing PAA solutions with various molar ratios of DAPOPPO/ODA. The specific example is as follows. In the reaction with a molar ratio of 1/9 (DAPOPPO/ODA), 26.20 g (0.077 mol) of DAPOPPO and 138.76 g (0.693 mol) of ODA were added into a flask with a stirrer, a nitrogen inlet, and a thermometer. Then 2000 mL of DMAc was poured into the flask and stirred until the solid absolutely dissolved. PMDA (167.95 g, 0.77 mol) was quickly added into the mixture, followed by adjusting the solid content to 15% (weight by weight) with DMAc. After stirring overnight, the isotropic solution was obtained. The other PAA solutions were prepared by the similar method, including homo-PAA and co-PAA. It was found that the viscosity of solution was too low to fabricate the fibers when the molar ratio of DAPOPPO/ODA was higher than 4/6. The corresponding polymerization route is depicted in Scheme 2.

Preparation of PI Fibers

The PI fibers were fabricated through a two-step method. Firstly, the preparation of PAA fibers was conducted by a dry-jet wet spinning process as shown in Scheme 3. After filtered and degassed at room temperature, the PAA solution

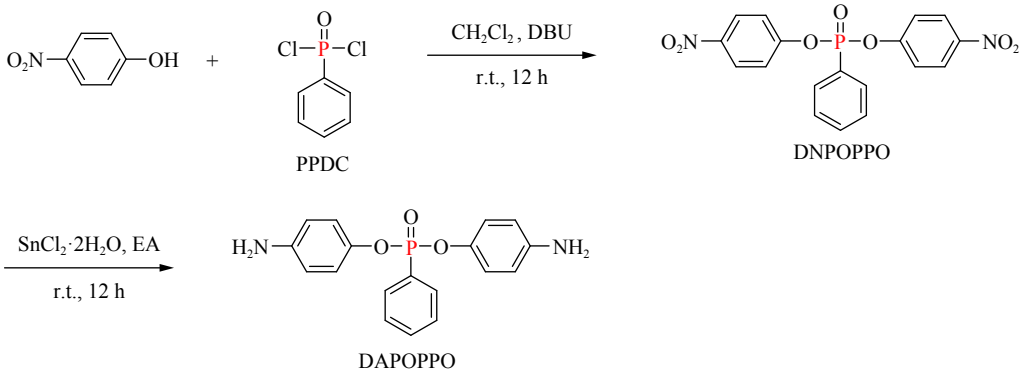

Scheme 1 Synthesis route to phosphorous-containing diamine DAPOPPO

https://doi.org/10.1007/s10118-019-2179-2

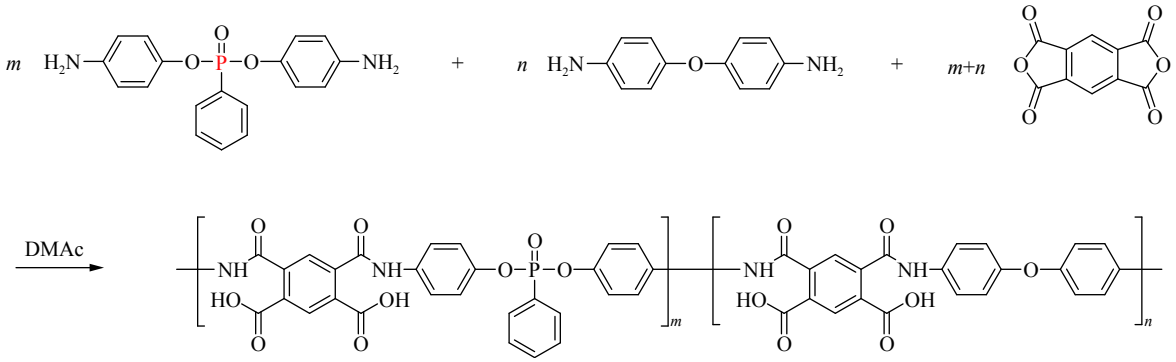

Scheme 2 Polymerization route to PAA solutions (ratio of *m*/*n* varied from 0/10 to 4/6)

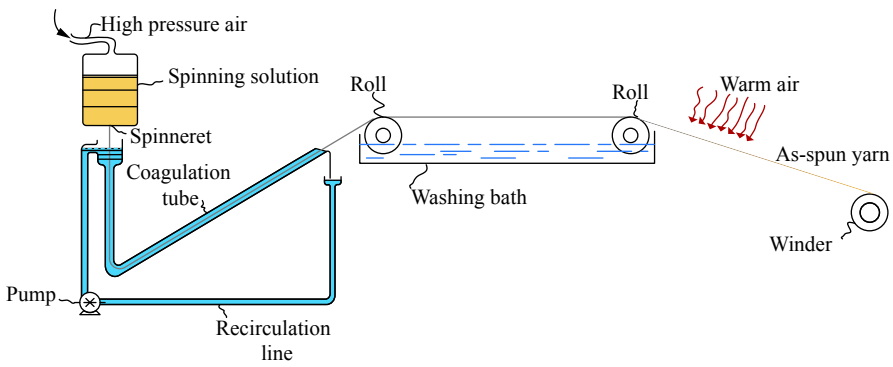

Scheme 3 Dry-jet wet spinning process of fabricating PAA fibers

was extruded into the coagulation bath to form a solidifying filament followed by entering into a second washing bath. Then, the solidifying filament was dried by heating tube and collected on the winder. As shown in Scheme 4, the PI fibers were finally obtained after thermal imidization and heat drawing.

Characterization

Fourier transform infrared (FTIR) measurement was carried out on a VERTEX 70 spectrometer with the scanning wavenumber in range of 400−4000 cm^{-1} at 32 scans. Nuclear magnetic resonance (NMR) spectroscopy was conducted on a Bruker 400 spectrometer at 400 MHz for ^{1}H-NMR, 162 MHz for ^{31}P-NMR, and 101 MHz for ^{13}C-NMR with tetramethylsilane as an internal standard. Melting points were determined on XT-4 melting point apparatus. Elemental analyses were carried out with an Elementar vario EL cube (Elementar Corporation, Germany). The inherent viscosity (η_{inh}) of PAA was measured using an Ubbelohde viscometer with a capillary inner diameter of 0.5 mm at the concentration of 0.5 $dL\cdot g^{-1}$ (dissolved in DMAc) at 30 °C. The mechanical properties of fibers were examined on a XQ-1 instrument with a gauge length of 20 mm and extension speed of 20 $mm\cdot min^{-1}$. For each group of fibers, at least 10 filaments were tested and the corresponding average value was used as the final representative in accordance with GB/T 14337. The surface morphologies of the PI fibers were viewed on a XL-30 scanning

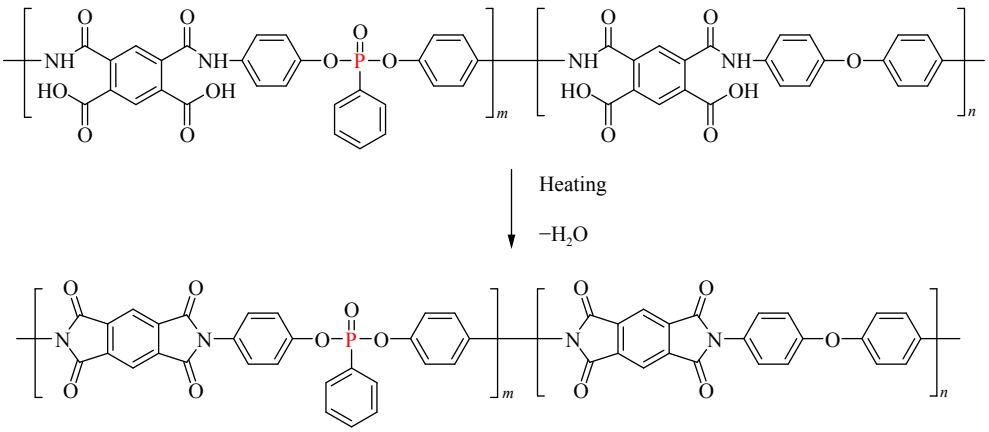

Scheme 4 The thermal imidization of PAA fibers

https://doi.org/10.1007/s10118-019-2179-2

electron microscope (SEM) FEG (FEI Company) and the samples were sprayed with Pt before observation. Dynamic mechanical analysis (DMA) was conducted on the Rheometric scientific DMTA-V instrument at 1 Hz and a heating rate of 10 °C·min^{-1} with the temperature ranging from 50 °C to 400 °C. Thermogravimetric analysis (TGA) was performed on TA Q50 instrument at a heating rate of 10 °C·min^{-1} from 30 °C to 850 °C under nitrogen atmosphere. AO exposure test was conducted in a ground-based AO effects simulation facility. The working air pressure was approximately 0.13–0.15 Pa. Discharge voltage and current were 200 V and 200 mA, respectively. PI fibers over 20 cm in length were placed on the sample tray in the vacuum chamber. Standard Kapton® films were used to calibrate exposure flux, and the final AO fluence was calculated from the mass loss of Kapton® by the following formula.[30,31]

$$F = \Delta M/\rho AE \quad (1)$$

where F is the total AO fluence (atoms·cm^{-2}), ΔM is the mass loss of Kapton® (g), ρ is the density of Kapton® (1.42 g·cm^{-3}), A is the exposure area of Kapton®, and E is the erosion constant of Kapton® (3×10^{-24} cm^3·atom^{-1}). Table S1 (in ESI) presents the AO fluence adopted in the current work.

RESULTS AND DISCUSSION

Synthesis and Characterization of Diamine Compound

Bis(4-aminophenoxy) phenyl phosphine oxide (DAPOPPO) was synthesized *via* a two-step route. As shown in Scheme 1, DNPOPPO was first obtained as an intermediate and the chemical structure was determined by FTIR. According to Fig. S1 (in ESI), the peak at 1438 cm^{-1} attributed to P—Ph groups was observed in FTIR spectra. Compared with the start material of *p*-nitrophenol, the peak at 3350 cm^{-1} associated with the bond of —OH disappeared. The results indicated DNPOPPO has been successfully synthesized. In the spectra of DAPOPPO, the bands of amine groups at 3435 and 3345 cm^{-1} emerged while those of nitro groups at 1550 and 1300 cm^{-1} disappeared. Moreover, other peaks arising from P=O (1256 cm^{-1}) and P—Ph (1438 cm^{-1}) were observed, confirming the maintaining of the phosphonate structure.

Preparation of PAA Solutions and PI Fibers

The inherent viscosities of PAA solutions with the diamine molar ratios of DAPOPPO/ODA varied from 0/10 to 4/6 are listed in Table 1. As can be seen, the inherent viscosity of PAA showed a decrease from 1.95 dL·g^{-1} to 1.80 dL·g^{-1} with increasing DAOPPO molar content from 0% to 40%. Actually, the charge density of the amino nitrogen decreased due to the electron-withdrawing effect of phosphorous element in DAPOPPO, which reduced the reactivity of nucleophilic reaction. When the molar ratio of DAPOPPO/ODA was increased to higher than 4/6, the viscosity of PAA solution was too low to extrude, and the fibers were unavailable.

All PI fibers were prepared from PAA fibers by thermal imidization and then the as-prepared PI fibers were drawn in heating tube to form the resulting PI fibers. The fibers were characterized by FTIR as shown in Fig. 1. In the spectra, the peaks at 1774 and 1720 cm^{-1} corresponded to the asymmetric and symmetrica stretching vibrations of C=O group. The peak at 1360 cm^{-1} belonged to the C—N stretching vibration of imide ring, and the peak at 734 cm^{-1} was ascribed to the bending vibration of imide ring. The absorption bands of PAA at 1712, 1652, and 1530 cm^{-1} corresponding to the groups of C=O (COOH), C=O (CONH), and C—NH, were not found, which indicated that all the PAA fibers were successfully converted into PI fibers. Notably, the intensity of peak at 1196 cm^{-1} attributed to P=O group showed an increase with increasing DAPOPPO content, which further indicated the successful preparation of co-PI fibers containing phosphate ester groups.

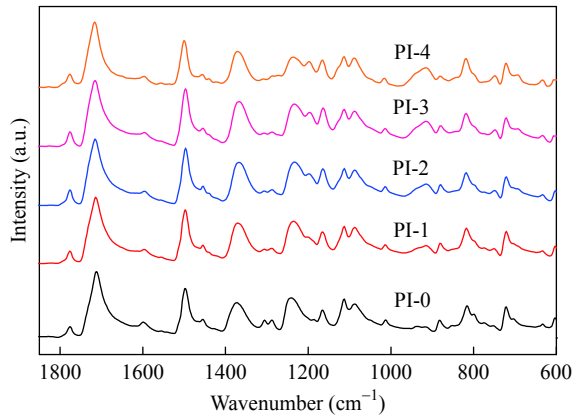

Fig. 1 FTIR spectra of co-PI fibers with different molar contents of DAPOPPO

Surface Morphologies of co-PI Fibers

The surface morphologies of PI fibers were observed by SEM. As shown in Fig. 2, all the fibers exhibited smooth surfaces and uniform diameters (15 μm) with complete cylindrical shapes. The results indicated that the fiber formation process in the coagulation bath was stable and the dual-diffusion process between the solvent and non-solvent was equilibrium.

Table 1 Inherent viscosities of PAA solutions and mechanical properties of co-PI fibers

Polymer	Diamine ratio (m:n)	Draft [a]/Draw [b] ratio	η_{inh} (dL·g^{-1})	Mechanical properties		
				Tensile strength (cN·dtex^{-1})	Initial modulus (cN·dtex^{-1})	Elongation at break (%)
PI-0	0:10	2.75/1.6	1.95	5.23 ± 0.44	79.65 ± 3.45	11.28 ± 0.51
PI-1	1:9	2.75/1.6	1.91	2.94 ± 0.19	60.13 ± 3.23	11.53 ± 0.48
PI-2	2:8	2.75/1.6	1.86	2.58 ± 0.24	56.01 ± 2.65	12.60 ± 0.49
PI-3	3:7	2.75/1.6	1.82	2.07 ± 0.27	53.66 ± 3.29	13.66 ± 0.43
PI-4	4:6	2.75/1.6	1.80	1.89 ± 0.13	51.28 ± 2.88	14.02 ± 0.53

[a] The ratio of the take-up speed to the extrusion speed; [b] The ratio of after-drawing speed to before-drawing speed passing the heat tube

https://doi.org/10.1007/s10118-019-2179-2

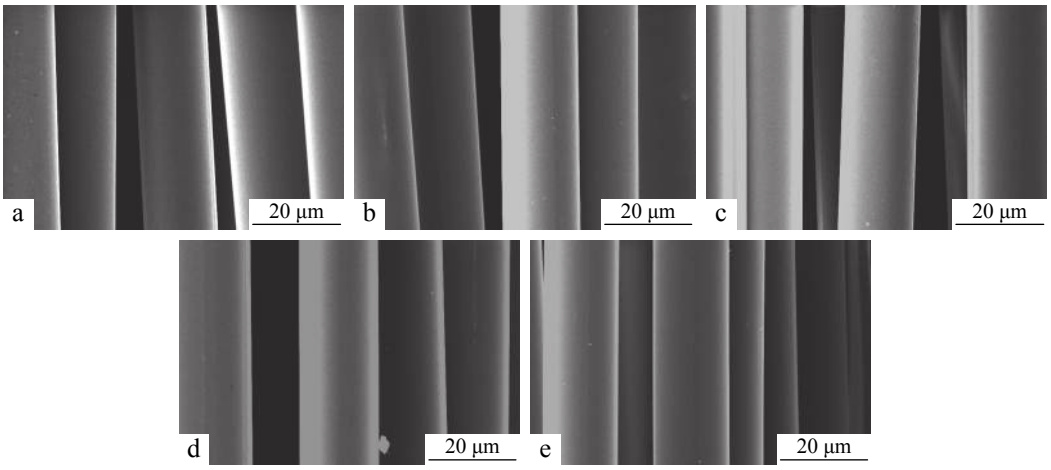

Fig. 2 Surface morphologies of PI fibers: (a) PI-0, (b) PI-1, (c) PI-2, (d) PI-3, (e) PI-4

Thermal Properties of PI Fibers

The glass transition temperatures (T_gs) of the fibers were measured by DMA as depicted in Fig. 3. The T_gs of PI-0, PI-1, PI-2, PI-3, and PI-4 were 400, 381, 360, 341, and 321 °C, respectively. Apparently, the incorporation of DAPOPPO caused decreasing T_gs of the fibers, because the flexibility of molecular segment was increased with more ester groups in DAPOPPO.

The thermal stabilities of co-PI fibers were investigated by TGA and the results are shown in Fig. 4. Obviously, the residues at 850 °C exhibited almost no change. The temperatures of 5% weight loss ($T_{5\%}$) were 573, 570, 560, 550, and 541 °C corresponding to PI-0, PI-1, PI-2, PI-3, and PI-4. The neat PI fiber exhibited the highest decomposition rate at 600 °C. However, the co-PI fibers showed two decomposition stages. The first one for the fibers at 522 °C was associated with the decomposition of P—C bond, whereas the second one at 600 °C was related to the decomposition of PI backbone, as shown in Fig. 4(b).

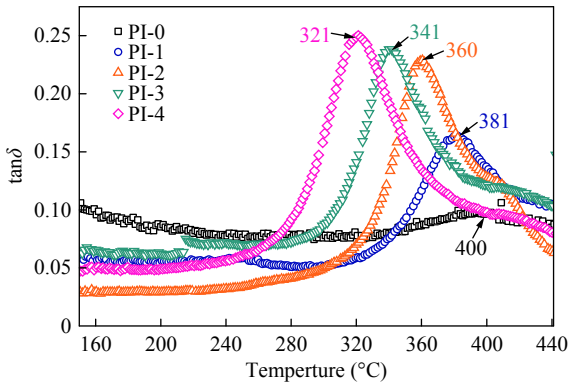

Fig. 3 tanδ versus temperature for PI fibers with different molar contents of DAPOPPO

Mechanical Properties of PI Fibers

Mechanical property was an important parameter for polymeric fibers in practical applications. As shown in Table 1 and Fig. 5, with the increase of DAPOPPO molar content, the tensile strength and initial modulus of the co-PI fibers decreased dramatically. However, the elongation at break improved significantly. Specifically, for the neat PI fiber, the tensile strength and initial modulus showed the values of 5.23 and 79.65 cN·dtex^{-1}, and elongation at break was 11.28%. For PI-1, PI-2, PI-3, and PI-4, the tensile strength and initial modulus were 2.94 and 60.13 cN·dtex^{-1}, 2.58 and 56.01 cN·dtex^{-1}, 2.07 and 53.66 cN·dtex^{-1}, and 1.89 and 51.28 cN·dtex^{-1}, respectively. Notably, the elongation at break showed the values of 11.53%, 12.60%, 13.66%, and 14.02%, corresponding to PI-1, PI-2, PI-3, and PI-4, respectively. Although the incorporation of more DAPOPPO into the PI chains led to decrease in mechanical properties of fibers, the tensile strength and initial modulus of fibers could still meet the requirements in protection fields.

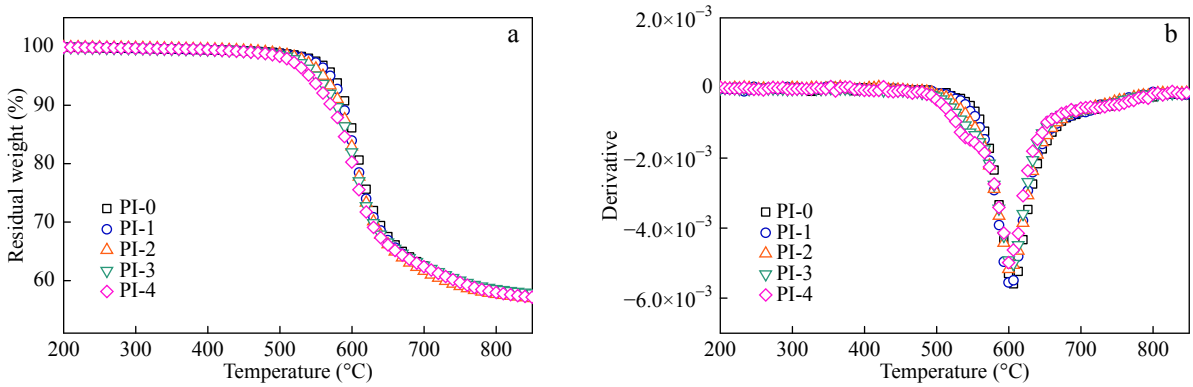

Fig. 4 (a) TGA and (b) DTG curves of PI fibers with different molar contents of DAPOPPO

https://doi.org/10.1007/s10118-019-2179-2

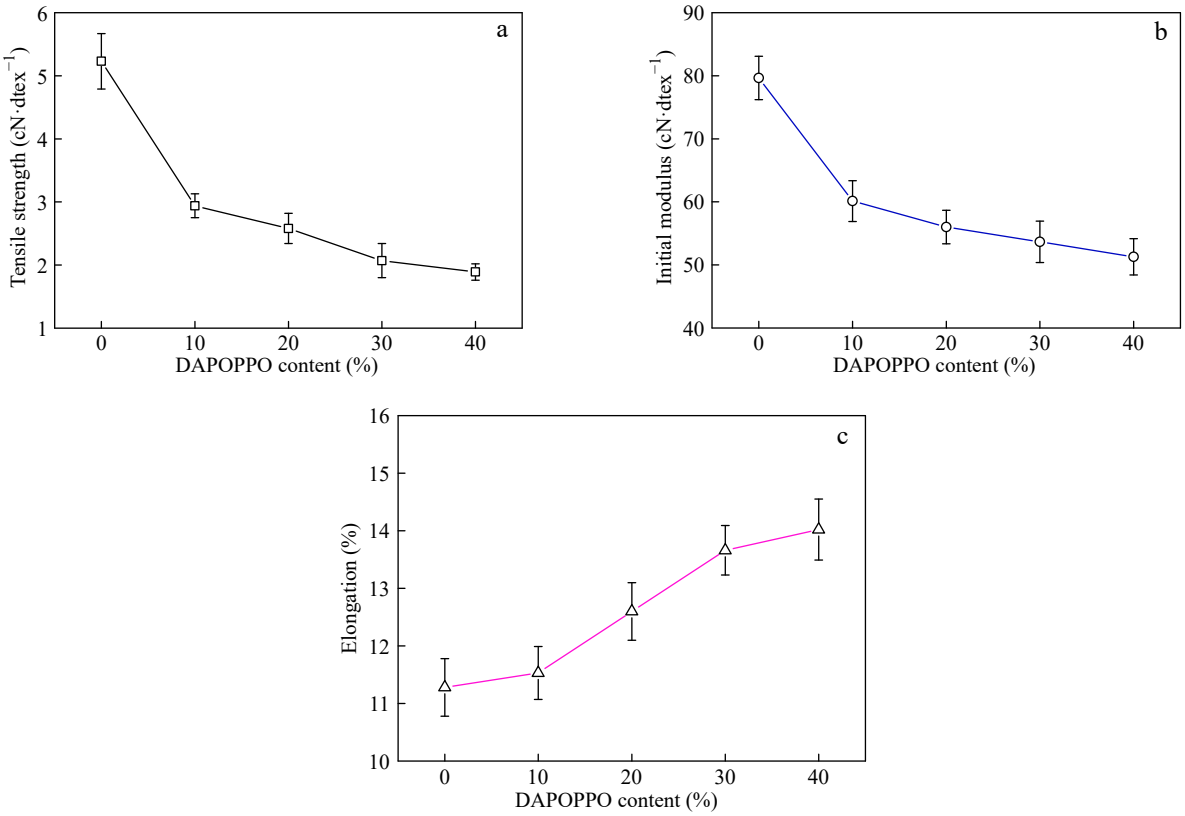

Fig. 5 Variation of mechanical properties with DAPOPPO molar content for PI fibers

Mass Loss of PI Fibers after AO Erosion

The co-PI fibers were exposed to simulated AO with fluences of 6.5×10^{19}, 1.3×10^{20}, 2.3×10^{20}, and 3.2×10^{20} atoms·cm^{-2} to investigate the AO resistance performance. When the polymer materials suffered AO attack, mass loss occurred. According to Table 2, with the AO fluences increasing from 6.5×10^{19} atoms·cm^{-2} to 3.2×10^{20} atoms·cm^{-2}, the mass loss of the fibers exhibited increases from 0.22 mg·cm^{-2} to 1.52 mg·cm^{-2}, from 0.16 mg·cm^{-2} to 0.90 mg·cm^{-2}, from 0.08 mg·cm^{-2} to 0.60 mg·cm^{-2}, associated with the fibers of PI-0, PI-2, and PI-4, respectively. Obviously, the mass loss of the fibers showed an increase with the AO fluences increase. At the same AO fluence, fiber with higher DAPOPPO content exhibited lower mass loss. Compared to PI-0, the fibers containing DAPOPPO showed excellent mass retention at higher AO fluence.

Surface Morphology and Composition of the Fibers after AO Erosion

As seen in Fig. 6, all the fibers showed smooth and uniform surface prior to AO erosion. When the fibers were exposed to AO beam, the surfaces became rough. At lower AO fluence, surface morphologies of all PI fibers showed no clear difference. However, when the AO fluence was increased to 2.2×10^{20} and 3.2×10^{20} atoms·cm^{-2}, PI-0 fiber showed obvious sparse, carpet-like appearance. As for the PI fibers containing DAPOPPO, the dense surface was observed, especially for PI-4 fibers. Consequently, the PI fibers with higher DAPOPPO content showed significant AO resistance even at higher AO fluence of 3.2×10^{20} atoms·cm^{-2}.

In order to investigate the surface element composition of fibers before and after AO erosion, XPS measurements were conducted. According to Table 3 and Fig. S3 (in ESI), O 1s, N 1s, and C 1s peaks existed in the XPS spectra of PI-0 fibers. P 2s and P 2p peaks appeared in the XPS spectra of PI-2 and PI-4 fibers, along with O 1s, N 1s, and C 1s peaks. When the fibers were exposed to AO, concentrations of C, N, and O showed no apparent change. However, an obvious increase in concentration of P was observed for the PI fibers containing DAPOPPO, *i.e.* PI-2 and PI-4. Specifically, the concentration of P showed an increase from 3.18% to 6.02%, and from 5.79% to 8.74% corresponding to PI-2 and PI-4, respectively. Moreover, the high-resolution XPS spectra of the C 1s and P 2p peaks associated with PI fibers before and after AO exposure were fitted. According to Table 4 and

Table 2 Mass loss of PI fibers versus AO exposure with difference fluence

Fiber	Diamine ratio (*m*:*n*)	SEM images No.	Mass loss [a] (mg·cm^{-2})			
			6.5×10^{19} atoms·cm^{-2}	1.3×10^{20} atoms·cm^{-2}	2.2×10^{20} atoms·cm^{-2}	3.2×10^{20} atoms·cm^{-2}
PI-0	0:10	0-a ~ 0-e	0.22	0.48	1.00	1.52
PI-2	2:8	2-a ~ 2-e	0.16	0.32	0.72	0.90
PI-4	4:6	4-a ~ 4-e	0.08	0.22	0.42	0.60

[a] Using Eq. (1) to calculate the total AO fluence with Kapton® film

https://doi.org/10.1007/s10118-019-2179-2

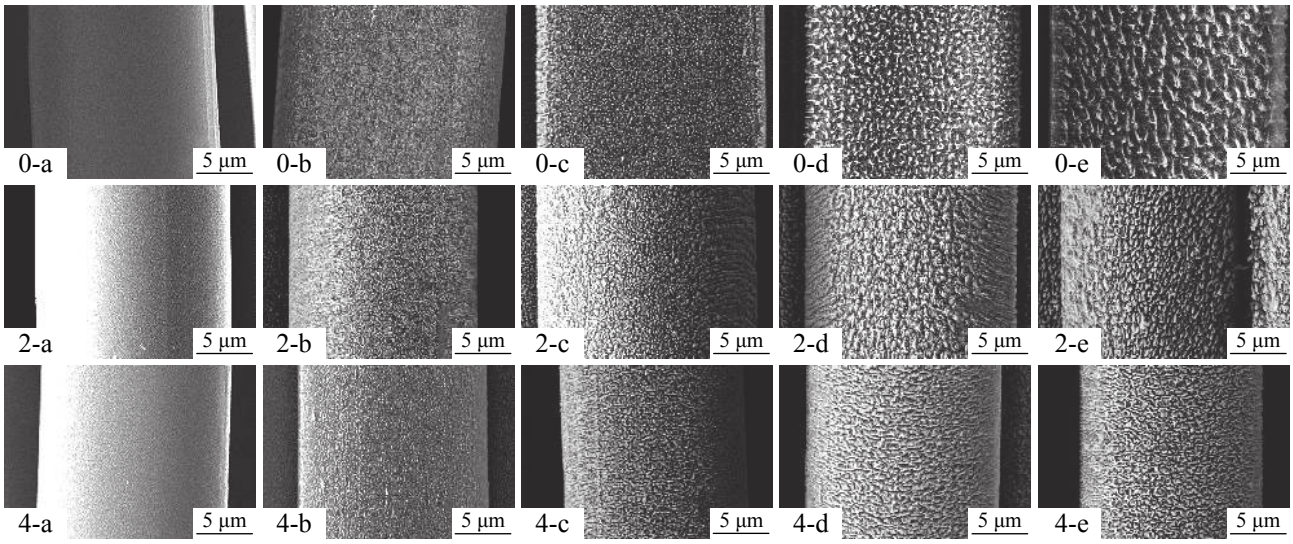

Fig. 6 Surface morphologies of co-PI fibers after erosion by AO beam with fluence of (a) 0, (b) 6.5×10^{19} atoms·cm^{-2}, (c) 1.3×10^{20} atoms·cm^{-2}, (d) 2.2×10^{20} atoms·cm^{-2}, and (e) 3.2×10^{20} atoms·cm^{-2}

Table 3 Surface element analysis before and after AO exposure

Element peaks	Element concentration (atoms%)					
	PI-0		PI-2		PI-4	
	Before AO	After AO	Before AO	After AO	Before AO	After AO
C 1s	67.69	68.62	60.00	59.00	53.53	50.26
O 1s	26.33	24.29	31.02	30.26	36.94	35.82
N 1s	5.98	7.09	5.80	4.27	3.75	5.18
P 2p	–	–	3.18	6.02	5.79	8.74

Fig. S4 (in ESI), the C 1s spectra were fitted by the C—C species at 284.8 eV binding energies (BEs), the C—N or C—O species at 287.6 eV BEs, and the C=O species at 289.0 eV BEs, which were ascribed to the carbon atoms of benzene rings, C—O—C in ODA or C—N—C in the imide ring, and C=O in the imide ring, respectively.[32] After AO exposure of PI-0, area of C—C species showed a decrease from 73.3% to 28.4%, whereas increases in those of C—N or C—O species and C=O species from 9.2% to 58.9% and 6.1% to 12.6% were observed. The similar surface composition variation of PI-4 appeared after AO exposure. The area of C—C species decreased from 40.7% to 17.67%, while area of those of C—N or C—O species and C=O species exhibited an increase from 39.9% to 67.9%, and from 19.4% to 30.2%. Notably, the area of P—(C_6H_5) at 133.3 eV BEs showed the value of 37.6% before AO exposure. However, when the fibers were exposed to AO, the P—(C_6H_5) peak disappeared, while the area of O=P at 134.6 eV BEs showed an obvious increase from 62.4% to 100% (Seen in Table 4 and Fig. S5 in ESI). The results indicated that C—C bond in the benzene ring of PI fibers was degraded to C—O bond, C—N bond or C=O bond after AO exposure. Consequently, carbon elements on the surface of fibers were oxidized by AO, which were released as volatiles. For the PI fibers containing PPO groups, P—(C_6H_5) bond was destroyed, and O=P bond formed after AO erosion. Therefore, the passivated phosphate layer deposited on the fiber surface, which effectively prevented fiber from AO erosion.

Mechanical Properties of the Fibers after AO Erosion

Fig. 7 shows the variations on tensile strength, initial modulus, and elongation at break of co-PI fibers under different AO fluence. With AO fluence increasing from 0 atom·cm^{-2} to

Table 4 Fitted relative content for C 1s, P 2p at high resolution

Element peaks		Before AO exposure			After AO exposure		
		BE (eV)	Assignments	Area (%)	BE (eV)	Assignments	Area (%)
PI-0	C 1s	283.2	–	11.4	–	–	–
		284.8	C—C	73.3	284.6	C—C	28.4
		287.2	C—N, C—O	9.2	285.4	C—N, C—O	58.9
		289.0	C=O	6.1	288.5	C=O	12.6
PI-4	C 1s	284.4	C—C	40.7	284.2	C—C	17.67
		285.8	C—N, C—O	39.9	285.1	C—N, C—O	67.9
		287.8	C=O	19.4	288.2	C=O	30.2
	P 2p	133.3	P—(C_6H_5)	37.6	–	–	–
		134.6	O=P	62.4	134.1	O=P	100

https://doi.org/10.1007/s10118-019-2179-2

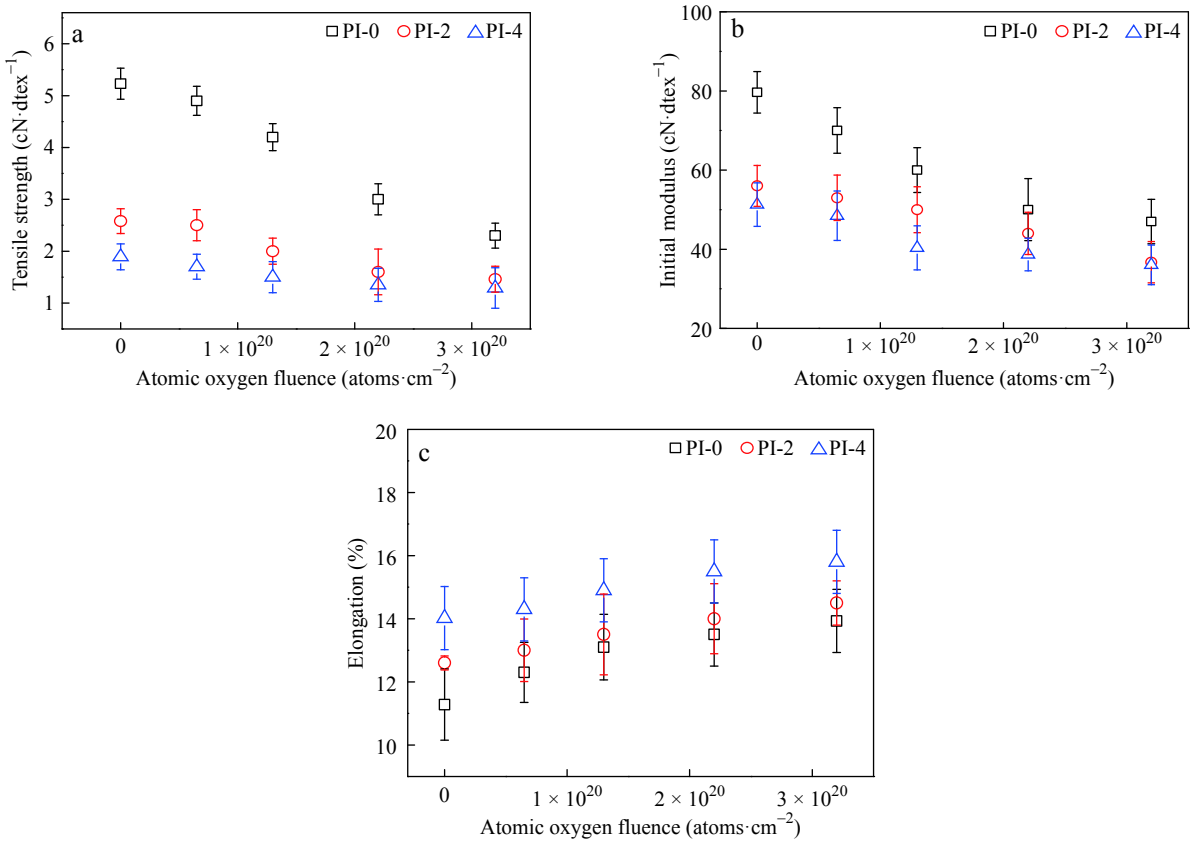

Fig. 7 Variation of (a) tensile strength, (b) initial modulus, and (c) elongation with AO fluence

3.2 × 10^{20} atoms·cm^{-2}, the tensile strengths of the PI fibers with DAPOPPO molar contents of 0%, 20%, and 40% showed decreases from 5.23 cN·dtex^{-1} to 2.30 cN·dtex^{-1}, 2.58 cN·dtex^{-1} to 1.50 cN·dtex^{-1}, and 1.89 cN·dtex^{-1} to 1.29 cN·dtex^{-1}, respectively. For the initial modulus of the co-PI fibers, the corresponding values declined from 79.65 cN·dtex^{-1} to 47.00 cN·dtex^{-1}, 56.01 cN·dtex^{-1} to 37.90 cN·dtex^{-1}, and 51.28 cN·dtex^{-1} to 35.90 cN·dtex^{-1} with increased AO fluence. Apparently, when the AO fluence was at 3.2 × 10^{20} atoms·cm^{-2}, the retention of tensile strength and initial modulus of the fibers increased from 44% to 68% and 59% to 70% with increased DAPOPPO molar contents from 0% to 40%. Consequently, the as-prepared PI fibers containing DAPOPPO showed prominent AO resistance.

CONCLUSIONS

In summary, a series of co-PI fibers intrinsically containing phosphorus were prepared *via* dry-jet wet spinning. The surface morphologies, thermal and mechanical properties, and AO resistance performance of the fibers were subsequently investigated. The results are concluded as follows.

The co-PI fibers exhibited smooth surface without defects. Although the incorporation of flexible DAPOPPO chains in PI chain caused T_g and $T_{5\%}$ to decrease, good thermal properties were kept for the fibers. With increasing DAPOPPO content from 0% to 40%, the mass loss of the fibers showed a significant decrease from 1.52 mg·cm^{-2} to 0.60 mg·cm^{-2} after AO erosion with the fluence of 3.2 × 10^{20} atoms·cm^{-2}. SEM results indicated that the PI fiber containing 40% DAPOPPO exhibited a denser surface, whereas the PI fiber without PPO group possessed a sparse carpet-like surface after AO erosion. The retentions of tensile strength and initial modulus at the AO fluence of 3.20 × 10^{20} atoms·cm^{-2} were improved dramatically from 44% to 68% and 59% to 70%, respectively. Actually, carbon elements on the surface of fibers were oxidized by AO, and the passivated phosphate layer deposited on the fiber surface after AO erosion, which effectively protected fiber from AO attack.

The excellent AO resistant performances make the co-PI fibers intrinsically containing PPO groups promising protective materials to apply in LEO.

Electronic Supplementary Information

Electronic supplementary information (ESI) is available free of charge in the online version of this article at http://dx.doi.org/10.1007/s10118-019-2179-2.

ACKNOWLEDGMENTS

This work was financially supported by the National Basic Research Program of China (973 Program, Key Project: No. 2014CB643604). We thank Beihang University for their help in AO experiment testing.

REFERENCES

1 Fischer, H. R.; Tempelaars, K.; Kerpershoek, A.; Dingemans, T.; Iqbal, M.; Lonkhuyzen, H. V.; Iwanowsky, B.; Semprimoschnig, C. Development of flexible LEO-resistant PI films for space applications using a self-healing mechanism by surface-directed phase separation of block copolymers. *ACS Appl. Mater. Interfaces* **2010**, *2*, 2218−2225.

2 Minton, T. K.; Wright, M. E.; Tomczak, S. J.; Marquez, S. A.; Shen, L.; Brunsvold, A. L.; Cooper, R.; Zhang, J.; Vij, V.; Guenthner, A. J.; Petteys, B. J. Atomic oxygen effects on POSS polyimides in low earth orbit. *ACS Appl. Mater. Interfaces* **2012**, *4*, 492−502.

3 Verker, R.; Grossman, E.; Eliaz, N. Erosion of POSS-polyimide films under hypervelocity impact and atomic oxygen: The role of mechanical properties at elevated temperatures. *Acta Mater.* **2009**, *57*, 1112−1119.

4 Liaw, D. J.; Wang, K. L.; Huang, Y. C.; Lee, K. R.; Lai, J. Y.; Ha, C. S. Advanced polyimide materials: Syntheses, physical properties and applications. *Prog. Polym. Sci.* **2012**, *37*, 907−974.

5 Sukhanova, T. E.; Baklagina, Y. G.; Kudryavtsev, V. V.; Maricheva, T. A.; Lednický, F. Morphology, deformation and failure behaviour of homo- and copolyimide fibres: 1. Fibres from 4,4′-oxybis(phthalic anhydride) (DPhO) and *p*-phenylenediamine (PPh) or/and 2,5-bis(4-aminophenyl)-pyrimidine (2,5PRM). *Polymer* **1999**, *40*, 6265−6276.

6 Cheng, Y.; Dong, J.; Yang, C.; Wu, T.; Zhao, X.; Zhang, Q. Synthesis of poly(benzobisoxazole-*co*-imide) and fabrication of high-performance fibers. *Polymer* **2017**, *133*, 50−59.

7 Niu, H.; Huang, M.; Qi, S.; Han, E.; Tian, G.; Wang, X.; Wu, D. High-performance copolyimide fibers containing quinazolinone moiety: Preparation, structure and properties. *Polymer* **2013**, *54*, 1700−1708.

8 Dong, J.; Yin, C.; Zhao, X.; Li, Y.; Zhang, Q. High strength polyimide fibers with functionalized graphene. *Polymer* **2013**, *54*, 6415−6424.

9 Chernik, V. N.; Novikov, L. S.; Bondarenko, G. G.; Gaidar, A. I.; Smirnova, T. N. Study of polymeric fiber erosion under oxygen plasma beams. *Bull. Russ. Acad. Sci.: Phys.* **2010**, *74*, 268−271.

10 Zhao, Y.; Li, G.; Dai, X.; Liu, F.; Dong, Z.; Qiu, X. AO-resistant properties of polyimide fibers containing phosphorous groups in main chains. *Chinese J. Polym. Sci.* **2016**, *34*, 1469−1478.

11 Liu, F.; Guo, H.; Zhao, Y.; Qiu, X.; Gao, L. Enhanced resistance to the atomic oxygen exposure of POSS/polyimide composite fibers with surface enrichment through wet spinning. *Eur. Polym. J.* **2018**, *105*, 115−125.

12 Tennyson, R. C. Protective coatings for spacecraft materials. *Sur. Coat. Techol.* **1994**, *68*, 519−527.

13 Deepa, D.; Packirisamy, S.; Korulla, R. M.; Ninan K. N. Atomic oxygen resistant coating from poly(tetramethyldisilylene-*co*-styrene). *J. Appl. Polym. Sci.* **2004**, *94*, 2368−2375.

14 Liu, B.; Ji, M.; Liu, J.; Fan, L.; Yang, S. Phenylphosphine oxide containing polyimide matrix resins for atomic oxygen-resistant fiber-reinforced composites. *High Perform. Polym.* **2013**, *25*, 907−917.

15 Atar, N.; Grossman, E.; Gouzman, I.; Bolker, A.; Murray, V. J.; Marshall, B. C.; Qian, M.; Minton, T. K.; Hanein, Y. Atomic-oxygen-durable and electrically-conductive CNT-POSS-polyimide flexible films for space applications. *ACS Appl. Mater. Interfaces* **2015**, *7*, 12047−12056.

16 Watson, K. A.; Palmieri, F. L.; Connell, J. W. Space environmentally stable polyimides and copolyimides derived from [2,4-bis(3-aminophenoxy)phenyl]diphenylphosphine oxide. *Macromolecules* **2002**, *35*, 4968−4974.

17 Connell, J. W.; Watson, K. A. Space environmentally stable polyimides and copolyimides derived from bis(3-aminophenyl)-3,5-di(trifluoromethyl)phenylphosphine oxide. *High Perform. Polym.* **2001**, *13*, 23−34.

18 Thompson, C. M.; Smith, J. G.; Connell, J. W. Polyimides prepared from 4,4′-(2-diphenylphosphinyl-1,4-phenylenedioxy)-diphthalic anhydride for potential space applications. *High Perform. Polym.* **2003**, *15*, 181−195.

19 Connell, J. W.; Smith, J. G.; Hedrick, J. L. Oxygen plasma-resistant phenylphosphine oxide-containing polyimides and poly(arylene ether heterocycle)s: 2. *Polymer* **1995**, *36*, 13−19.

20 Smith, J. G.; Connell, J. W.; Hergenrother, P. M. Oxygen plasma resistant phenylphosphine oxide-containing poly(arylene ether)s. *Polymer* **1994**, *35*, 2834−2839.

21 Jeong, K. U.; Kim, J. J.; Yoon, T. H. Synthesis and characterization of novel polyimides containing fluorine and phosphine oxide moieties. *Polymer* **2001**, *42*, 6019−6030.

22 Zhu, Y.; Zhao, P.; Cai, X.; Meng, W.; Qing, F. Synthesis and characterization of novel fluorinated polyimides derived from bis[4-(4′-aminophenoxy)phenyl]-3,5-bis(trifluoromethyl)phenyl phosphine oxide. *Polymer* **2007**, *48*, 3116−3124.

23 Wei, J. H.; Gang, Z. X.; Ming, L. Q.; Rehman, S.; Wei, Z. H.; Dong, D. G.; Hai, C. C. Atomic oxygen resistant phosphorus-containing copolyimides derived from bis[4-(3-aminophenoxy)phenyl] phenylphosphine oxide. *Polym. Sci. Ser. B* **2014**, *56*, 788−798.

24 Li, Z.; Liu, J.; Gao, Z.; Yin, Z.; Fan, L.; Yang, S. Organo-soluble and transparent polyimides containing phenylphosphine oxide and trifluoromethyl moiety: Synthesis and characterization. *Eur. Polym. J.* **2009**, *45*, 1139−1148.

25 Zhao, Y.; Dong, Z.; Li, G.; Dai, X.; Liu, F.; Ma, X.; Qiu, X. Atomic oxygen resistance of polyimide fibers with phosphorus-containing side chains. *RSC Adv.* **2017**, *7*, 5437−5444.

26 Zhao, Y.; Feng, T.; Li, G.; Liu, F.; Dai, X.; Dong, Z.; Qiu, X. Synthesis and properties of novel polyimide fibers containing phosphorus groups in the main chain. *RSC Adv.* **2016**, *6*, 42482−42494.

27 Zhao, Y.; Li, G.; Liu, F.; Dai, X.; Dong, Z.; Qiu, X. Synthesis and properties of novel polyimide fibers containing phosphorus groups in the side chain (DATPPO). *Chinese J. Polym. Sci.* **2017**, *35*, 372−385.

28 Liu, Y. L.; Hsiue, G. H.; Lee, R. H.; Chiu, Y. S. Phosphorus-containing epoxy for flame retardant. III: Using phosphorylated diamines as curing agents. *J. Appl. Polym. Sci.* **1997**, *63*, 895−901.

29 Ding, X.; Qiu, X.; Ma, X.; Li, G.; Gao, L. Preparations and properties of the phosphoruscontaining polyimide fibers. *Chem. J. Chinese U.* **2013**, *11*, 2650−2654.

30 Miyazaki, E.; Tagawa, M.; Yokota, K.; Yokota, R.; Kimoto, Y.; Ishizawa, J. Investigation into tolerance of polysiloxane-block-polyimide film against atomic oxygen. *Acta Astronaut.* **2010**, *66*, 922−928.

31 Shimamura, H.; Nakamura, T. Mechanical properties degradation of polyimide films irradiated by atomic oxygen. *Polym. Degrad. Stab.* **2009**, *94*, 1389−1396.

32 Duo, S. W.; Li, M. S.; Zhou, Y. C.; Tong, J. Y.; Sun, G. Investigation of surface reaction and degradation mechanism of Kapton during atomic oxygen exposure. *J. Mater. Sci. Technol.* **2003**, *19*, 535−539.

https://doi.org/10.1007/s10118-019-2179-2